188 *Organometallics* **2001,** *20,* 188−198

Syntheses, Structures, and Reactivities of Heterobimetallic Bridging Dinitrogen Complexes Containing Group 6 and Group 4 or 5 Transition Metals[1]

Hiroshige Ishino, Tatsuya Nagano, Shigeki Kuwata, Youhei Yokobayashi, Youichi Ishii,* and Masanobu Hidai*,†

Department of Chemistry and Biotechnology, Graduate School of Engineering, The University of Tokyo, Hongo, Bunkyo-ku, Tokyo 113-8656, Japan

Yasushi Mizobe

Institute of Industrial Science, The University of Tokyo, Roppongi, Minato-ku, Tokyo 106-8558, Japan

Received August 8, 2000

A series of heterobimetallic dinitrogen complexes containing group 6 and group 4 or 5 transition metals were synthesized by the reaction of the tungsten or molybdenum dinitrogen complexes *cis*-$[W(N_2)_2(PMe_2Ph)_4]$ (**1**) and *trans*-$[M(N_2)_2(dppe)_2]$ (**2**) (M = W, Mo) with group 4 or group 5 compounds such as $[CpTiCl_3]$, $[Cp_2M'Cl_2]$ (M′ = Ti, Zr, Hf), or $[Cp'M'Cl_4]$ (Cp′ = Cp, Cp*; M′ = Nb, Ta). Crystallographic studies of the complexes thus obtained including $[WCl(PMe_2Ph)_4(\mu\text{-}N_2)TiCpCl_2]$ and $[WCl(PMe_2Ph)_4(\mu\text{-}N_2)NbCpCl_3]$ revealed that the M−N−N−M′ core is essentially linear, and the N−N bond is regarded to have the formal bond order of 2. Several μ-N_2 complexes with methyl ligands at the group 4 or 5 metal center were also obtained through the reaction of dinitrogen complexes **1** and **2a** (M = W) with the methyl complexes $[Cp_2ZrMeCl]$, $[TaMe_3Cl_2]$, and $[NbMe_2Cl_3]$. The reaction of the complex $[WCl(dppe)_2(\mu\text{-}N_2)TiCpCl_2]$ with Li_2S_5 afforded the η^2-pentasulfido complex $[WCl(dppe)_2(\mu\text{-}N_2)TiCpS_5]$, where the η^2-S_5 ligand forms a six-membered chelate ring with the chair conformation. Protonation of the μ-N_2 complexes having PMe_2Ph ligands gave NH_3 in moderate yield, concurrent with the formation of a small amount of NH_2NH_2.

Introduction

Activation and chemical transformation of molecular dinitrogen at metal centers under mild conditions have been the subject of current attention.[2−7] In particular, recent advances in the studies on the active site of nitrogenase[8] have aroused intense interest in properties and reactivities of dinitrogen bound at multinuclear transition metal centers, and intriguing reactivities of multinuclear μ-N_2 complexes have been found which include the N−N fission.[9−12] However, most of the μ-N_2 complexes investigated so far are homobimetallic compounds, and the chemistry of heterobimetallic dinitrogen complexes still remains to be explored. In fact, the structurally characterized μ-N_2 complexes containing two different transition metals have been very limited in number.[11,13−19]

In the course of our continuous study on reactivities of the molybdenum and tungsten dinitrogen complexes such as *cis*-$[W(N_2)_2(PMe_2Ph)_4]$ (**1**) and *trans*-$[M(N_2)_2(dppe)_2]$ (dppe = $Ph_2PCH_2CH_2PPh_2$) (**2a**, M = W; **2b**, M = Mo), we have previously found that the coordinated dinitrogen in this type of tungsten complexes is attacked by Lewis acids including not only group 13 metal (B,[20]

---

† Present address: Department of Materials Science and Technology, Faculty of Industrial Science and Technology, Science University of Tokyo, Noda, Chiba 278-8510, Japan. E-mail: hidai@mail.rs.noda.sut.ac.jp.

(1) Preparation and Properties of Molybdenum and Tungsten Dinitrogen Complexes. 70. Part 69: Nishibayashi, Y.; Takemoto, S.; Iwai, S.; Hidai, M. *Inorg. Chem.*, in press.

(2) Hidai, M.; Mizobe, Y. *Chem. Rev.* **1995**, *95*, 1115−1133.

(3) Gambarotta, S. *J. Organomet. Chem.* **1995**, *500*, 117−126.

(4) Bazhenova, T. A.; Silov, A. E. *Coord. Chem. Rev.* **1995**, *95*, 69−145.

(5) Hidai, M.; Mizobe, Y. In *Molybdenum Enzymes, Cofactors and Model Systems*; Stiefel, E. I., Coucouvanis, D., Newton, W. E., Eds.; American Chemical Society: Washington, DC, 1993; pp 346−362.

(6) Leigh, G. J. *Acc. Chem. Res.* **1992**, *25*, 177−181.

(7) Hidai, M.; Mizobe, Y. In *Reactions of Coordinated Ligands*; Braterman, P. S., Ed.; Plenum Press: New York, 1989; Vol. 2, pp 53−114.

(8) Howard, J. B.; Rees, D. C. *Chem. Rev.* **1996**, *96*, 2965−2982.

(9) Caselli, A.; Solari, E.; Scopelliti, R.; Floriani, C.; Re, N.; Rizzoli, C.; Chiesi-Villa, A. *J. Am. Chem. Soc.* **2000**, *122*, 3652−3670.

(10) Clentsmith, G. K. B.; Bates, V. M. E.; Hitchcock, P. B.; Cloke, G. N. *J. Am. Chem. Soc.* **1999**, *121*, 10444−10445.

(11) Peters, J. C.; Cherry, J.-P. F.; Thomas, J. C.; Baraldo, L.; Mindiola, D. J.; Davis, W. M.; Cummins, C. C. *J. Am. Chem. Soc.* **1999**, *121*, 10053−10067.

(12) Berno, P.; Gambarotta, S. *Angew. Chem., Int. Ed. Engl.* **1995**, *34*, 822−824.

(13) Mindiola, D. J.; Meyer, K.; Cherry, J.-P. F.; Baker, T. A.; Cummins, C. C. *Organometallics* **2000**, *19*, 1622−1624.

(14) O'Donoghue, M. B.; Davis, W. M.; Schrock, R. R.; Reiff, W. M. *Inorg. Chem.* **1999**, *38*, 243−252.

(15) O'Donoghue, M. B.; Zanetti, N. C.; Davis, W. M.; Schrock, R. R. *J. Am. Chem. Soc.* **1997**, *119*, 2753−2754.

(16) Schrock, R. R.; Kolodziej, R. M.; Liu, A. H.; Davis, W. M.; Vale, M. G. *J. Am. Chem. Soc.* **1990**, *112*, 4338−4345.

(17) Cradwick, P. D.; Chatt, J.; Crabtree, R. H.; Richards, R. L. *J. Chem. Soc., Chem. Commun.* **1975**, 351−352.

(18) Mercer, M. *J. Chem. Soc., Dalton Trans.* **1974**, 1637−1640.

(19) Mercer, M.; Crabtree, R. H.; Richards, R. L. *J. Chem. Soc., Chem. Commum.* **1973**, 808−809.

(20) Ishino, H.; Ishii, Y.; Hidai, M. *Chem. Lett.* **1998**, 677−678.

10.1021/om000684j CCC: $20.00
Publication on Web 12/02/2000

Al,[21] Ga[22]) compounds but also group 4 metal (Ti, Zr, Hf) complexes[23] to afford the μ-N_2 complexes. Treatment of **1** with [Cp_2TiCl_2] (Cp = η^5-C_5H_5) or [Cp_2MCl_2]/NaI (M = Zr, Hf) affords the heterobimetallic bridging dinitrogen complexes [$WX(PMe_2Ph)_4(\mu$-$N_2)MCp_2Cl$] (**3a**, M = Ti, X = Cl; **3b**, M = Zr, X = I; **3c**, M = Hf, X = I) in good yield. We have now extended this study to the reactions of complexes **1** and **2** with other group 4 and 5 transition metal complexes. Here we describe synthesis, characterization, and some reactivities of a series of heterobimetallic dinitrogen complexes in which the μ-N_2 ligand bridges group 6 and group 4 or 5 metal centers.

Results and Discussion

Synthesis of Group 4−Group 6 Heterobimetallic Bridging Dinitrogen Complexes. In the previous communication,[23] we reported that [Cp_2TiCl_2] shows moderate reactivity toward complex **1** at 50 °C to give the heterobimetallic bridging dinitrogen complex **3a** in good yield. [Cp_2MCl_2] (M = Zr, Hf) also reacts with **1** in the presence of NaI to form analogous μ-N_2 complexes **3b** and **3c**. The crystallographically determined molecular structure of [$WI(PMe_2Ph)_3(py)(\mu$-$N_2)ZrCp_2Cl$] (**3b′**, py = pyridine) derived from **3b** and pyridine revealed the linear W(μ-N_2)Zr core with the formal $(N_2)^{2-}$ ligand. To expand the scope of this synthetic method for heterobimetallic μ-N_2 complexes, we turned our attention to the mono-Cp complex [$CpTiCl_3$], which is expected to have higher reactivity toward dinitrogen complexes owing to its strong Lewis acidic nature. When complex **1** was allowed to react with an equimolar amount of [$CpTiCl_3$] in benzene at room temperature, rapid reaction took place to form the heterodinuclear μ-N_2 complex [$WCl(PMe_2Ph)_4(\mu$-$N_2)TiCpCl_2$] (**4**), which was isolated in good yield after recrystallization (eq 1). The IR spectrum of **4** showed a medium absorption at 1408 cm^{-1} characteristic of the ν(NN) band, suggesting that the N−N bond has a double bond character, and **4** may be viewed as the formal $(N_2)^{2-}$-bridged W(II)−Ti(IV) complex. It is to be noted that the ν(NN) value of complex **4** is considerably lower than that (1468 cm^{-1}) of complex **3a**.[23] Substitution of the 15e⁻ fragment $TiCp_2Cl$ in **3a** with the 11e⁻ fragment $TiCpCl_2$ causes stronger π-donation from the N_2 ligand to the titanium atom, which is reflected in the lower ν(NN) value. The ^1H NMR and ^{31}P NMR spectra showed a broad Me singlet at δ 1.63 and a singlet with ^{183}W satellites (J_{WP} = 277 Hz) at δ −24.5, respectively, indicating the trans configuration of the chloride and μ-N_2 ligands around the tungsten center. Attempted reactions of **1** with [Cp^*TiCl_3] (Cp* = η^5-C_5Me_5), [$CpZrCl_3$], [Cp^*ZrCl_3], or [Cp^*HfCl_3] failed to give any isolable heterobimetallic μ-N_2 complexes.

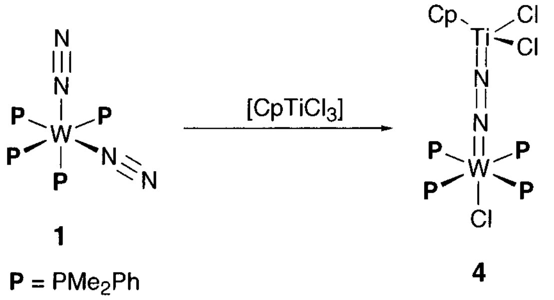

(1)

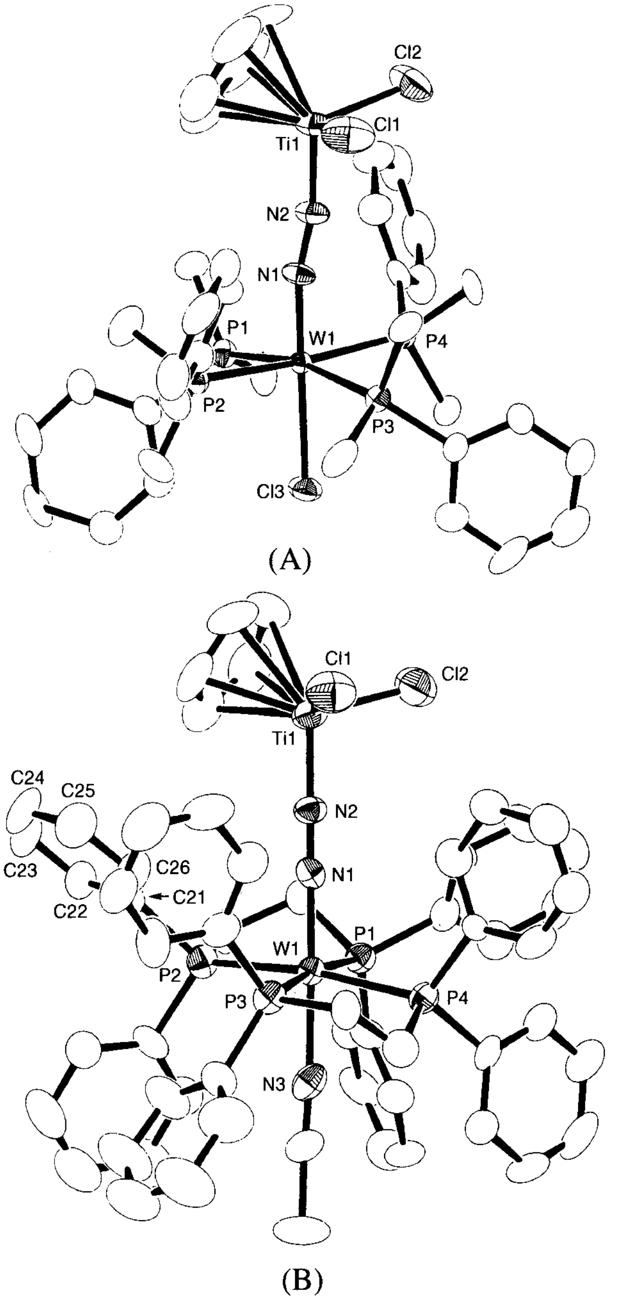

Figure 1. Molecular structures of **4** (A) and **9a**·$3CH_2Cl_2$ (B). Solvating CH_2Cl_2 molecules and hydrogen atoms are omitted for clarity. Thermal ellipsoids are shown at the 50% probability level.

The molecular structure of complex **4** was unambiguously determined by X-ray diffraction study (Figure 1). Selected bond distances and angles are collected in Table 1, and an ORTEP drawing is given in Figure 1. In accordance with the spectral data, complex **4** has an octahedral configuration around the tungsten center with the mutually trans μ-N_2 and chloride ligands, and the titanium center adopts a typical three-legged piano

---

[21] Takahashi, T.; Kodama, T.; Watakabe, A.; Uchida, Y.; Hidai, M. *J. Am. Chem. Soc.* **1983**, *105*, 1680−1681.

[22] Takagahara, K.; Ishino, H.; Ishii, Y.; Hidai, M. *Chem. Lett.* **1998**, 897−898.

[23] Mizobe, Y.; Yokobayashi, Y.; Oshita, H.; Takahashi, T.; Hidai, M. *Organometallics* **1994**, *13*, 3764−3766.

Table 1. Selected Bond Distances and Angles in 4 and 9a·3CH$_2$Cl$_2$

	4 (X = Cl(3))	**9a**·3CH$_2$Cl$_2$ (X = N(3))
	Distances (Å)	
W(1)−N(1)	1.782(5)	1.85(1)
N(1)−N(2)	1.270(8)	1.21(2)
Ti(1)−N(2)	1.792(5)	1.82(1)
W(1)−P(1)	2.525(6)	2.483(4)
W(1)−P(2)	2.523(5)	2.489(5)
W(1)−P(3)	2.513(6)	2.533(4)
W(1)−P(4)	2.509(5)	2.516(5)
Ti(1)−Cl(1)	2.313(3)	2.299(6)
Ti(1)−Cl(2)	2.317(3)	2.307(6)
	Angles (deg)	
W(1)−N(1)−N(2)	166(1)	178(1)
X−W(1)−N(1)	176.8(5)	178.4(6)
Ti(1)−N(2)−N(1)	168.8(8)	179(1)
P(1)−W(1)−N(1)	97.7(5)	88.4(4)
P(2)−W(1)−N(1)	86.4(5)	87.2(4)
P(3)−W(1)−N(1)	94.4(5)	97.4(4)
P(4)−W(1)−N(1)	88.9(5)	100.7(4)

stool structure. The W−N−N−Ti array in **4** is almost linear, and this type of linear structure is ubiquitous in dinuclear μ-N$_2$ complexes.[2,24] The core structure is closely related to that of the previously reported W−Zr complex **3b′**.[23] The Ti−N distance at 1.792(5) Å is shorter than that found in the Mo−Ti μ-N$_2$ complex [(Ph^{t}BuN)$_3$Ti(μ-N$_2$)Mo{N^{t}Bu(3,5-Me$_2$C$_6$H$_3$)}$_3$] (1.880(3) Å)[11] but is in the range of Ti−N double bond distances found in titanium amido complexes such as [TiCl$_2${η^5:η^1-C$_5$H$_4$(CH$_2$)$_3$N^{i}Pr}] (1.867(2) Å),[25] [Cp*Ti(NMe$_2$)(CH$_2$Ph)$_2$] (1.887(2) Å),[26] and [CpTiCl$_2$(NPPh$_3$)] (1.78(1) Å).[27] The W−N distance at 1.782(5) Å also indicates a multiple-bonding character as found in complex **3b′**. The N−N bond distance of 1.270(8) Å is slightly longer than those of the above-mentioned Mo−Ti complex (1.229(4) Å) and **3b′** (1.24(2) Å), and the N$_2$ fragment in **4** may be viewed as a formal (N$_2$)$^{2-}$ ligand which acts as a four-electron donor to each of the tungsten and titanium centers.

Although the dinitrogen complexes with dppe ligands **2** are unreactive toward [Cp$_2$TiCl$_2$], they react smoothly with [CpTiCl$_3$]. Thus, when the tungsten complex **2a** was treated with an equimolar amount of [CpTiCl$_3$] at room temperature, [WCl(dppe)$_2$(μ-N$_2$)TiCpCl$_2$] (**5a**), the dppe analogue of **4**, was isolated in good yield. The spectral data of **5a** including the IR absorption at 1412 cm^{-1} attributable to the ν(NN) vibration are consistent with the formulation. The ^{1}H NMR signal of the Cp ligand appeared in the high-field region (δ 5.70) compared with those of **3a** (δ 6.30) and **4** (δ 6.44), which is accounted for by the shielding effect of a phenyl group of the dppe ligands located nearby (vide infra). The molybdenum dinitrogen complex **2b** similarly reacted with [CpTiCl$_3$] to give the analogous Mo−Ti complex [MoCl(dppe)$_2$(μ-N$_2$)TiCpCl$_2$] (**5b**).

Complex [Cp$_2$Ti(OTf)$_2$] (OTf = OSO$_2$CF$_3$) was also effective for the synthesis of μ-N$_2$ W−Ti complexes from either **1** or **2a**, and [W(OTf)(PMe$_2$Ph)$_4$(μ-N$_2$)TiCp$_2$(OTf)] (**6a**) or [W(OTf)(dppe)$_2$(μ-N$_2$)TiCp$_2$(OTf)] (**6b**) was obtained, respectively. The low electroconductivitiy of **6a** and **6b** (6.6 S cm^2 mol^{-1} for **6a** and 6.9 S cm^2 mol^{-1} for **6b** in CH$_2$Cl$_2$) implies that they are essentially nonelectrolytes with coordinated OTf ligands. It should be noted that treatment of chloro complexes such as **3a** or **5a** with AgOTf failed to give the corresponding OTf derivatives.

The anionic dinitrogen complex *trans*-[NBu$_4$][W(NCS)(N$_2$)(dppe)$_2$] (**7**) readily derived from complex **2a** shows higher reactivities toward electorophiles than **2a**, which is substantiated in the reactions with fluoroarene complexes.[28,29] As expected, complex **7** smoothly reacted with [Cp$_2$MCl$_2$] (M = Ti, Zr, Hf) and [Cp′TiCl$_3$] (Cp′ = Cp, Cp*) at room temperature to give [W(NCS)(dppe)$_2$(μ-N$_2$)MCp$_2$Cl] (**8a**, M = Ti; **8b**, M = Zr; **8c**, M = Hf) and [W(NCS)(dppe)$_2$(μ-N$_2$)TiCp′Cl$_2$] (**9a**, Cp′ = Cp; **9b**, Cp′ = Cp*), respectively (eq 2). The IR spectra of **8a**−**c** showed strong absorptions at 2049−2056 cm^{-1} and medium absorptions at 1545−1559 cm^{-1} attributable to the ν(NCS) and ν(NN) bands, respectively, while the ν(NN) values for **9a** (1441 cm^{-1}) and **9b** (1433 cm^{-1}) were considerably lower (vide supra). The ^{1}H NMR and ^{31}P NMR spectra also agreed well with the formulation.

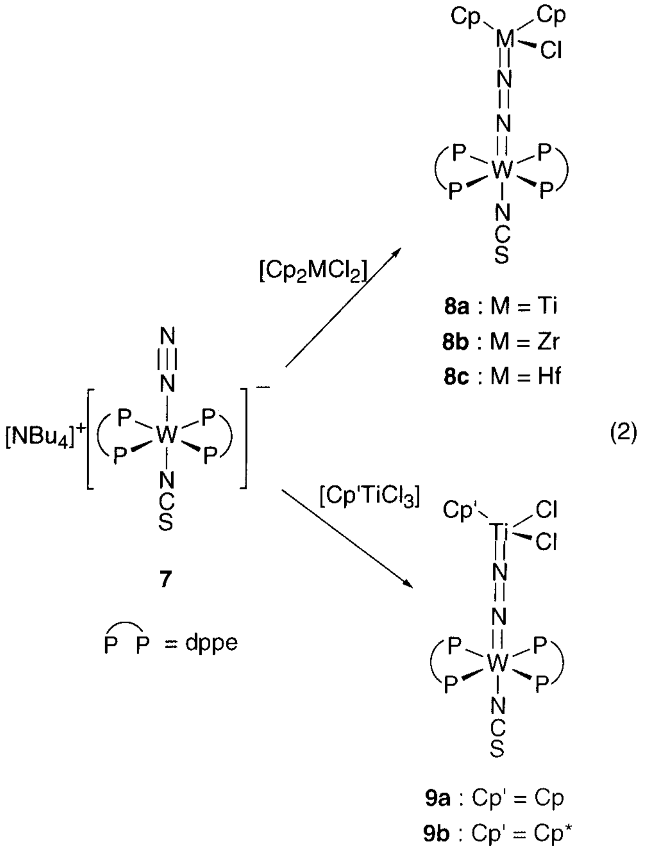

The molecular structure of **9a**·3CH$_2$Cl$_2$ was confirmed crystallographically. As shown in Figure 1, the structure around the dinuclear core of **9a** is closely related to that of **4** except that the W(1)−N(1) and Ti(1)−N(2) bonds in **9a** are slightly elongated, while the N(1)−N(2) bond distance is shorter than that in **4**. The CpTi moiety is situated in the vicinity of one of the dppe phenyl rings

---

(24) Henderson, R. A. *Transition Met. Chem.* **1990**, *15*, 330−336.

(25) Sinnema, P.-J.; Veen, L.; Spek, A. L.; Veldman, N.; Teuben, J. H. *Organometallics* **1997**, *16*, 4245−4247.

(26) Sinnema, P.-J.; Spaniol, T. P.; Okuda, J. *J. Organomet. Chem.* **2000**, *598*, 179−181.

(27) Latham, I. A.; Leigh, G. J.; Huttner, G.; Jibril, I. *J. Chem. Soc., Dalton Trans.* **1986**, 377−383.

(28) Ishii, Y.; Kawaguchi, M.; Ishino, Y.; Aoki, T.; Hidai, M. *Organometallics* **1994**, *13*, 5062−5071.

(29) Ishii, Y.; Ishino, Y.; Aoki, T.; Hidai, M. *J. Am. Chem. Soc.* **1992**, *114*, 5429−5430.

Table 2. Selected Bond Distances and Angles in $\mathbf{10a}\cdot CH_2Cl_2\cdot Et_2O$ and $\mathbf{10d}\cdot$2MeCN

	10a·$CH_2Cl_2\cdot Et_2O$ (M = Nb)	**10d**·2MeCN (M = Ta)
	Distances (Å)	
W(1)−N(1)	1.785(7)	1.783(7)
N(1)−N(2)	1.254(9)	1.275(9)
M(1)−N(2)	1.852(7)	1.857(8)
M(1)−Cl(1)	2.492(3)	2.462(3)
M(1)−Cl(2)	2.434(3)	2.446(3)
M(1)−Cl(3)	2.481(3)	2.449(3)
	Angles (deg)	
W(1)−N(1)−N(2)	176.0(6)	173.5(6)
Cl(4)−W(1)−N(1)	176.4(2)	173.5(6)
M(1)−N(2)−N(1)	179.1(6)	174.2(7)

(C(21)−C(26)). Such conformation is required to accommodate the bulky CpTi group and explains the observation that the Cp protons of the μ-N_2 complexes with dppe ligands resonate in a higher field region (δ 5.6−5.9) than those of the PMe_2Ph analogues (δ 6.1−6.5). In contrast with the above reactions, [Cp*$ZrCl_3$] did not react with complex **7**, and [Cp$ZrCl_3$] or [Cp*$HfCl_3$] gave the W(I) dinitrogen complex *trans*-[W(NCS)(dppe)$_2$(N_2)][30] as the only characterized product.

Synthesis of Group 5−Group 6 Heterobimetallic Bridging Dinitrogen Complexes. Synthesis of a series of W−Nb and W−Ta μ-N_2 complexes was also examined to compare the reactivities of the group 4−group 6 and group 5−group 6 heterobimetallic μ-N_2 complexes. When complex **1** was allowed to react with [Cp′MCl_4] (M = Nb, Ta; Cp′ = Cp, Cp*) in benzene at room temperature, the μ-N_2 complexes [WCl(PMe_2Ph)$_4$(μ-N_2)MCp′Cl_3] (**10a**, M = Nb, Cp′ = Cp; **10b**, M = Nb, Cp′ = Cp*; **10c**, M = Ta, Cp′ = Cp; **10d**, M = Ta, Cp′ = Cp*) were formed in high yield (eq 3). The ^{1}H NMR spectra of **10a**−**d** showed a broad singlet assignable to the PMe protons, and the ^{31}P{^{1}H} NMR spectra exhibited a singlet with ^{183}W satellites. In the IR spectra, medium absorptions attributable to the ν(NN) band were observed at 1385−1435 cm^{-1}, where the ν(NN) values of the W−Nb complexes **10a** and **10b** are lower than those of the W−Ta analogues **10c** and **10d** by ca. 40 cm^{-1}.

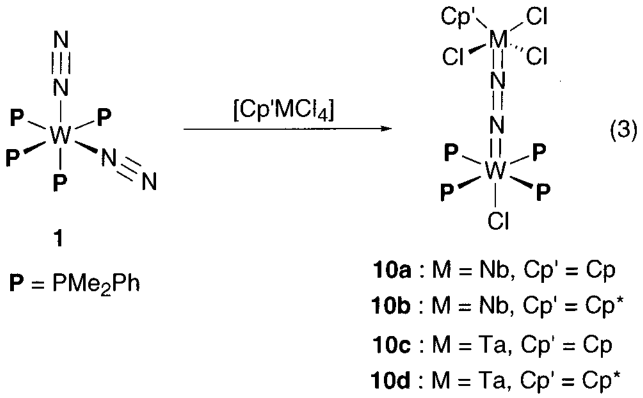

The molecular structures of complex **10a**·$CH_2Cl_2\cdot Et_2O$ and **10d**·2MeCN were unambiguously determined by X-ray diffraction study. Selected bond distances and angles are listed in Table 2, and their ORTEP drawings are depicted in Figure 2. In agreement with the spectral data, the tungsten centers in **10a** and **10d** have an octahedral configuration with the mutually trans μ-N_2 and chloro ligands, and the niobium and tantalum centers take a square pyramidal geometry with the Cp′ ligand at the apex. The W−N−N−Nb and W−N−N−Ta arrays are almost linear, as observed in **3b′**, **4**, and **9a**·3CH_2Cl_2. The N−N bond distances (1.254(9) Å for **10a**·$CH_2Cl_2\cdot Et_2O$ and 1.275(9) Å for **10d**·2MeCN) are

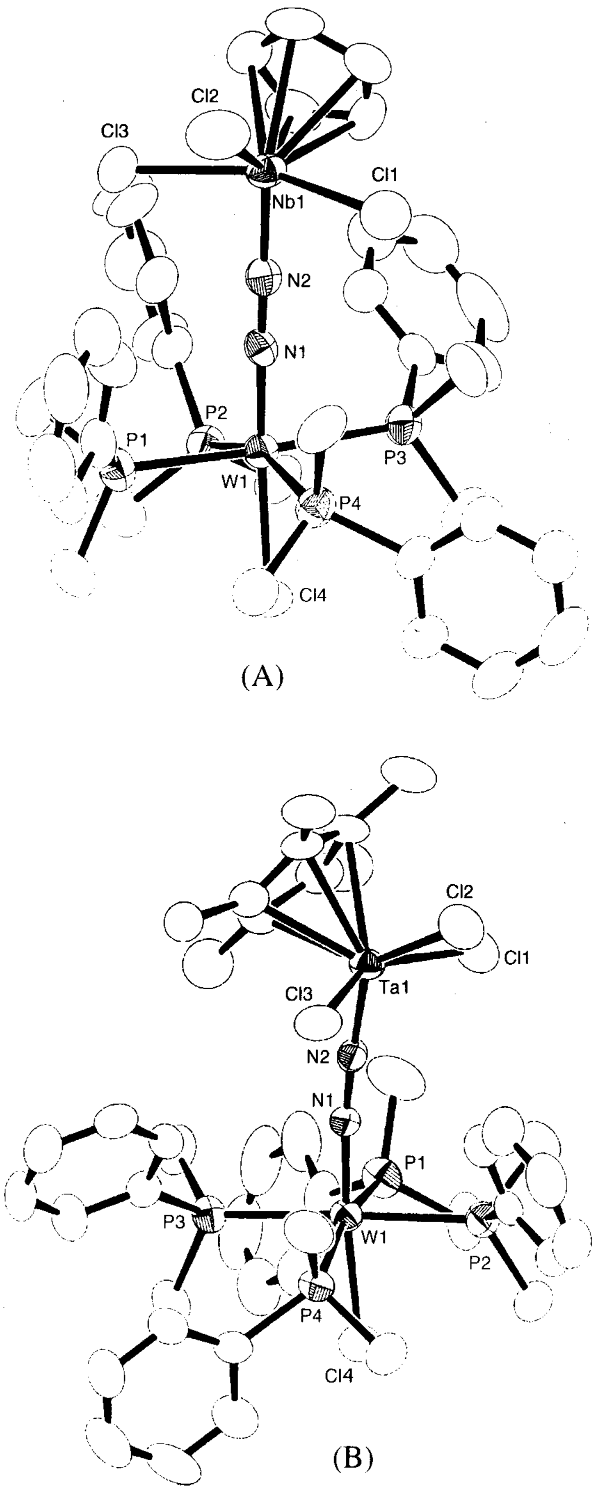

Figure 2. Molecular structures of **10a**·$CH_2Cl_2\cdot Et_2O$ (A) and **10d**·2MeCN (B). Solvating ether and MeCN molecules and hydrogen atoms are omitted for clarity. Thermal ellipsoids are shown at the 50% probability level.

---

[30] Chatt, J.; Leigh, G. J.; Neukomm, H.; Pickett, C. J.; Stanley, D. R. *J. Chem. Soc., Dalton Trans.* **1980**, 121−127.

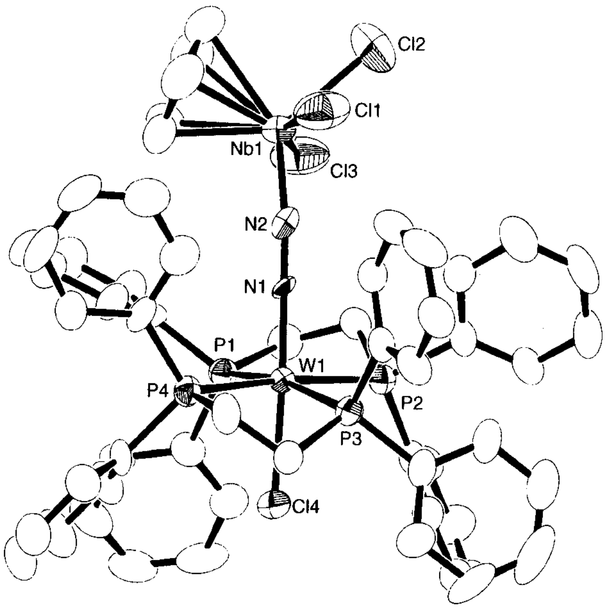

Figure 3. Molecular structure of **11a**·Et_2O. Solvating ether molecule and hydrogen atoms are omitted for clarity. Thermal ellipsoids are shown at the 50% probability level. Selected bond distances (Å) and angles (deg): W(1)−N(1), 1.806(8); N(1)−N(2), 1.25(1); Nb(1)−N(2), 1.868(9); 2.467(4); W(1)−N(1)−N(2), 171.1(8); Nb(1)−N(2)−N(1), 175.0(8).

close to that of **4** and correspond to the bond order of 2. Thus, the oxidation state of the diamagnetic metal centers in these complexes may be assigned to be W(II)−M(V) (M = Nb, Ta). Crystallographically characterized heterobimetallic dinitrogen complexes containing group 5 metals have not been known until very recently. The Mo−V and Mo−Nb complexes [$\{[(Me_3SiNCH_2CH_2)_3N]Mo(\mu\text{-}N_2)\}_2VCl(THF)$] (N−N, 1.217(7) and 1.221(7) Å)[14] and [$\{(3,5\text{-}Me_2C_6H_3)^tBuN\}_3Mo(\mu\text{-}N_2)Nb\{N^iPr(C_6H_3Me_2\text{-}3,5)\}_3$] (N−N, 1.235(10) Å)[13] have been considered as formal $(N_2)^{2-}$ complexes, and their N−N distances are compared well with those found for **10a** and **10d**.

Complexes **2a** and **7** also gave analogous μ-N_2 complexes [$WCl(dppe)_2(\mu\text{-}N_2)MCpCl_3$] (**11a**, M = Nb; **11b**, M = Ta) and [$W(NCS)(dppe)_2(\mu\text{-}N_2)MCpCl_3$] (**12a**, M = Nb; **12b**, M = Ta) in good yield on reactions with [$CpMCl_4$] (M = Nb, Ta). However, they failed to react with [Cp^*MCl_4] probably due to steric reasons. The molecular structure of **11a**·Et_2O established by crystallographic study is given in Figure 3. The structure around the dinuclear core is closely related to that of **10a**.

Reactions of the Heterobimetallic Dinitrogen Complexes with Unsaturated Compounds. Metal−nitrogen multiple bonds have been known to undergo interesting reactions with unsaturated compounds including the [2+2] cycloaddition to form a metallacycle.[31−33] Aiming at developing new coupling reactions of the μ-N_2 ligand and organic unsaturated compounds, reactions of complexes **4**, **5a**, **6a**, **10a**, **10d**, **11a**, and **11b** with various alkenes, alkynes, CO, and isocyanides were examined. Unfortunately, however, most of the attempted reactions yielded a complex mixture of uncharacterized products. Only in the reaction of **10d** with ^tBuNC (5 equiv) at 50 °C did substitution of one PMe_2Ph ligand on the tungsten atom take place to form [$WCl(PMe_2Ph)_3(^tBuNC)(\mu\text{-}N_2)TaCp^*Cl_3$] (**13**) in moderate yield. Complex **13** showed a ν(CN) absorption at 2112 cm^{-1} as well as a ν(NN) absorption at 1458 cm^{-1}, and the ^1H and $^{31}P\{^1H\}$ NMR data suggest the *mer* arrangement of the PMe_2Ph ligands. It should also be mentioned that complex **10d** did not undergo ligand substitution with pyridine or 2,2′-bipyridine, although one of the PMe_2Ph ligands in the W−Zr complex **3b** was readily displaced by pyridine to give **3b′**.

Synthesis of Bridging Dinitrogen Complexes with Alkyl Ligands. Attempts to introduce methyl ligands to the dinuclear cores of the μ-N_2 complexes **4**, **5a**, **6a**, **9a**, **10a**, **10c**, **11a**, or **11b** by reactions with MeLi or MeMgBr resulted in the reduction of the tungsten center to give the parent dinitrogen complexes **1** and **2a** as the only characterizable product. Use of other alkylmetals such as Me_2Zn and Me_4Sn was not successful either. However, several μ-N_2 complexes with alkyl ligands were obtained through the reaction of the dinitrogen complexes **1**, **2**, and **7** with [$Cp_2ZrMeCl$], [Me_3TaCl_2], or [Me_2NbCl_3].

Although the reaction of **1** with [$Cp_2ZrMeCl$] did not proceed in the absence of NaI, addition of excess NaI effectively promoted the reaction to give the μ-N_2 complex [$WI(PMe_2Ph)_4(\mu\text{-}N_2)ZrCp_2Me$] (**14a**). The IR spectrum of **14a** showed a medium ν(NN) band at 1541 cm^{-1}, and the Me signal in its ^1H NMR appeared as a singlet at δ 0.37. In contrast with the reaction of **1**, the anionic dinitrogen complex **7** reacted with [$Cp_2ZrMeCl$] in the absence of NaI to form [$W(NCS)(dppe)_2(\mu\text{-}N_2)ZrCp_2Me$] (**14b**). This complex exhibited a singlet at δ −0.02 in the ^1H NMR spectrum attributable to the Zr−Me group. The molecular structure of **14b** confirmed by crystallographic study is shown in Figure 4. The Zr(1)−C(1) distance at 2.342(8) Å is not unusual, and other metrical features are similar to those observed in **3b′**.

On the other hand, treatment of **1** and **2** with [Me_3TaCl_2] afforded [$WCl(PMe_2Ph)_4(\mu\text{-}N_2)TaMe_3Cl$] (**15a**) and [$MCl(dppe)_2(\mu\text{-}N_2)TaMe_3Cl$] (**15b**, M = W; **15c**, M = Mo), respectively, in moderate yield. In the ^1H NMR spectra, the Me signals of these complexes were observed as a singlet at δ 0.45, 0.23, and 0.13, respectively, and the spectrum of **15b** showed essentially no temperature dependence over the range 20 to −60 °C. A structure having a trigonal bipyramidal tantalum center with the chloro and μ-N_2 ligands at the apical positions is consistent with the spectral data, but we must await further investigation to clarify the detailed structure of **15**. Similarly, complexes **2** reacted with [Me_2NbCl_3] to produce [$MCl(dppe)_2(\mu\text{-}N_2)NbMe_2Cl_2$] (**16a**, M = W; **16b**, M = Mo). Complexes **14**−**16** are thermally stable up to 70 °C, and migration of the Me group from the metal to the μ-N_2 ligand has not been observed so far.

Reaction of the Heterobimetallic Dinitrogen Complexes with Li_2S_5. In relevalence to the active site of nitrogenase, great interest has been focused on multimetallic dinitrogen complexes having sulfur-based ligands, although examples of such complexes are still

---

(31) Blake, R. E.; Antonelli, D. M.; Henling, L. M.; Schaefer, W. P.; Hardcastle, K. I.; Bercaw, J. E. *Organometallics* **1998**, *17*, 718−725.

(32) Fairfax, D.; Stein, M.; Livinghouse, T.; Jensen, M. *Organometallics* **1997**, *16*, 1523−1525.

(33) Walsh, P. J.; Hollander, F. J.; Bergman, R. G. *Organometallics* **1993**, *12*, 3705−3723.

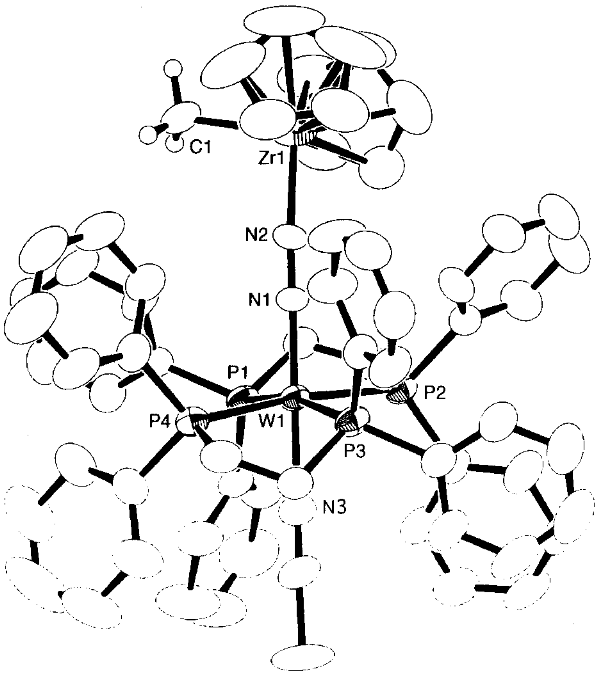

Figure 4. Molecular structure of **14b**. Hydrogen atoms except for the Zr−CH_3 hydrogens are omitted for clarity. Thermal ellipsoids are shown at the 50% probability level. Selected bond distances (Å) and angles (deg): W(1)−N(1), 1.850(5); N(1)−N(2), 1.223(7); Zr(1)−N(2), 2.042(6); Zr(1)−C(1), 2.342(8); W(1)−N(1)−N(2), 173.6(5); Zr(1)−N(2)−N(1), 174.6(5); C(1)−Zr(2)−N(2), 98.4(3).

limited.[34−36] Having a series of heterobimetallic μ-N_2 complexes in hand, we next investigated their reactions with sulfur ligands. When complex **5a** was treated with Li_2S_5 in THF at room temperature, the μ-N_2 complex with the pentasulfido ligand [WCl(dppe)$_2$(μ-N_2)TiCpS$_5$] (**17**) was isolated in good yield (eq 4). However, attempted reactions of **4**, **10a**, or **11a** with Li_2S_5 and of **5a** with Li_2S, Li_2S_2, or $[NH_4]_2[WS_4]$ led to uncharacterized mixtures. The ^{1}H and ^{31}P NMR spectra of **17** were comparable to those of **5a**, and the IR spectrum of **17** showed a medium ν(NN) absorption at 1406 cm^{-1}, which is slightly lower than that of **5a**. These spectral data indicate that the core structure of **5a** was maintained during the reaction with Li_2S_5.

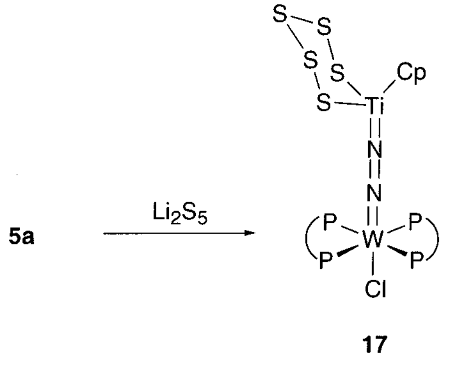

(4)

17

Table 3. Selected Bond Distances and Angles in 17·1.5Et$_2$O

Distances (Å)			
W(1)−N(1)	1.799(8)	N(1)−N(2)	1.247(9)
Ti(1)−N(2)	1.827(9)	Ti(1)−S(1)	2.406(4)
Ti(1)−S(5)	2.374(4)	S(1)−S(2)	2.055(5)
S(2)−S(3)	2.033(6)	S(3)−S(4)	2.050(6)
S(4)−S(5)	2.053(5)		
Angles (deg)			
W(1)−N(1)−N(2)	176.5(7)	Cl(1)−W(1)−N(1)	177.1(3)
Ti(1)−N(2)−N(1)	172.6(7)	S(1)−Ti(1)−N(2)	97.1(3)
S(5)−Ti(1)−N(2)	98.2(3)	Ti(1)−S(1)−S(2)	102.1(2)
Ti(1)−S(5)−S(4)	100.4(2)	S(1)−S(2)−S(3)	105.8(2)
S(2)−S(3)−S(4)	106.5(2)	S(3)−S(4)−S(5)	105.1(2)

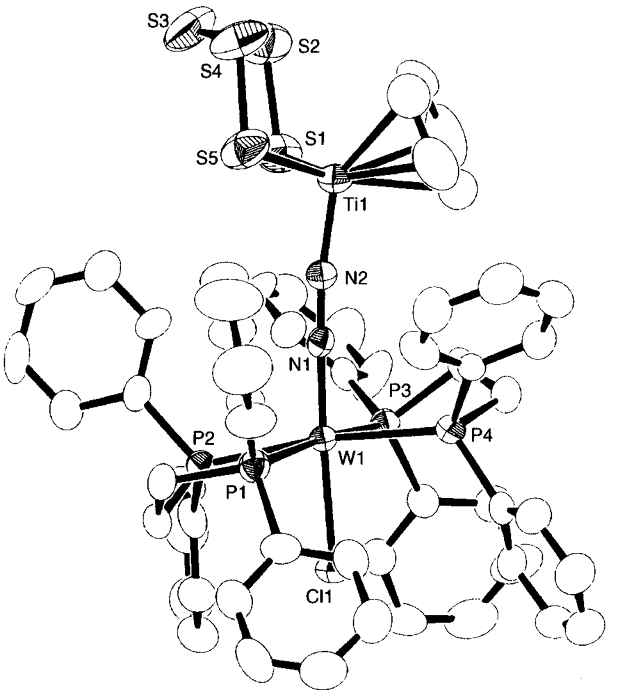

Figure 5. Molecular structures of **17**·1.5Et$_2$O. Solvating ether molecules and hydrogen atoms are omitted for clarity. Thermal ellipsoids are shown at the 50% probability level.

The molecular structure of complex **17**·1.5Et$_2$O was confirmed by an X-ray diffraction study. Selected bond distances and angles are summarized in Table 3, and an ORTEP drawing is given in Figure 5. In agreement with the spectral data, complex **17** has a linear W−N−N−Ti core with the N−N bond distance at 1.247(9) Å. The η^2-pentasulfido ligand is bonded to the Ti atom to form a six-membered ring with the chair conformation, and the CpTiS$_5$ fragment takes the structure that minimizes the steric congestion with the dppe ligands on the tungsten atom. The distances of the Ti−S (2.406(4), 2.374(4) Å) and S−S (2.033(6)−2.055(5) Å) bonds are comparable with those found in other titanium polysulfido complexes including [Cp$_2$TiS$_5$].[37,38] Investigation into the reactivity of **17** is now in progress.

Protonation of Heterobimetallic Dinitrogen Complexes with H_2SO_4. The protonation of coordinated dinitrogen to form NH_3 or NH_2NH_2 requires the concomitant transfer of six or four electrons, respectively, from the metal center. Therefore, as far as mononuclear

---

[34] O'Regan, M. B.; Liu, A. H.; Finch, W. C.; Schrock, R. R.; Davis, W. M. *J. Am. Chem. Soc.* **1990**, *112*, 4331−4338.

[35] Henderson, R. A.; Morgan, S. H. *J. Chem. Soc., Dalton Trans.* **1990**, 1107−1109.

[36] Schrock, R. R.; Wesolek, M.; Liu, A. H.; Wallace, K. C.; Dewan, J. C. *Inorg. Chem.* **1988**, *27*, 2050−2054.

[37] Müller, E. G.; Petersen, J. L.; Dahl, L. F. *J. Organomet. Chem.* **1976**, *111*, 91−112.

[38] Epstein, E. F.; Bernal, I. *J. Organomet. Chem.* **1971**, *26*, 229−245.

Table 4. Protonation of Bridging Dinitrogen Ligands Forming Ammonia and/or Hydrazine[a]

complex	yield of NH_3 (%)[a]	yield of NH_2NH_2 (%)[a]
3a[b]	43	8
3b[b]	17	16
4	36	2
10a	44	6
10b	34	2
10c	29	9
10d	41	0
15a	23	10

[a] Based on total nitrogen in the N_2 complex. Reaction conditions: heterobimetalic dinitrogen complex (0.050−0.100 mmol); H_2SO_4 (10 equiv); MeOH (3 mL); room temperature; 3 h; under Ar. [b] See ref 23.

dinitrogen complexes are concerned, such conversion is expected to occur effectively only with complexes of highly electron-rich metal centers such as complex **1**, where all the electrons are provided from the single metal. On the other hand, the conversion of coordinated dinitrogen to nitrogen hydrides on multimetallic complexes is presumed to require less electrons per one metal atom, and more diversified metals are expected to effect such reactions. In fact, it has been demonstrated that various types of multinuclear dinitrogen complexes yield NH_3 and NH_2NH_2 on protonolysis under mild conditions.[2]

To gain information about the chemical properties of dinitrogen activated by the group 4 or 5−group 6 metal pairs, we have investigated the protonation reactions with H_2SO_4. Representative results are summarized in Table 4 together with the values for **3a** and **3b** reported previously.[23] As observed with **3a** and **3b**, the heterobimetallic μ-N_2 complexes with PMe_2Ph ligands, **4**, **10a**−**d**, and **15a**, gave NH_3 in 23−44% yield, while NH_2NH_2 was formed in lower yield (0−10%). Essentially no N_2 gas evolution was observed. Unfortunately, we could not characterize the metal products, and the fate of nitrogen is not fully understood. On the other hand, complexes having dppe ligands (**5a**, **5b**, **8b**, **8c**, **11a**, and **11b**) gave much lower yields of NH_3 (0−6%) and NH_2NH_2 (0−1%), and considerable amounts of the starting complexes were recovered. It should be pointed out that NH_2NH_2 is most commonly observed as the major nitrogen hydride product in the protonation of homobimetallic μ-N_2 complexes.[2] In addition, protonolysis of heterodinuclear μ-N_2 complexes has not been studied extensively. It has been reported that treatment of the W−Ta complex $[Cp^*WMe_3(\mu\text{-}N_2)TaCp^*Me_2]$ with HOTf gives the mononuclear tungsten hydrazido(1−) complex $[Cp^*Me_3W(\eta^2\text{-}NHNH_2)][OTf]$ and $[Cp^*TaMe_2(OTf)_2]$,[39] while the hydrolysis of the Re−Cr complex $[ReCl(PMe_2Ph)_4(\mu\text{-}N_2)CrCl_3(THF)_2]$ results in the formation of $[ReCl(N_2)(PMe_2Ph)_4]$.[40] In contrast, the reaction of the Mo−W μ-N_2 complex $[Cp^*MoMe_3(\mu\text{-}N_2)WCp^*Me_3]$ with HCl affords NH_3 in 16% yield based on the total nitrogen.[16] In the protonation reactions of the heterobimetallic μ-N_2 complexes derived from **1**, the group 4 or 5 fragment seems to have minor effects on the NH_3/NH_2NH_2 selectivity, although the mechanism of the protonation and N−N bond cleavage at the dinuclear cores is still unclear.

Finally, reduction of the μ-N_2 complexes **4**, **5a**, **10a**, and **10b** with sodium or magnesium was also examined, since the conversion of μ-N_2 complexes to the corresponding nitrides in the presence[9,10,11,13] or absence[41−43] of alkali metals has recently been established. However the only characterized products were the parent dinitrogen complexes **1** and **2a**.

Concluding Remarks

We have succeeded in the systematic synthesis of a series of heterobimetallic dinitrogen complexes containing group 6 and group 4 or 5 transition metals. The synthetic method established in this study provides an important approach to the chemistry of dinitrogen activated by two different metal centers, which still remains much less developed in comparison with the chemistry of homodinuclear dinitrogen complexes. The spectroscopic and structural properties of the μ-N_2 complexes newly prepared were examined in detail, revealing that the μ-N_2 moiety is best regarded as a formal $(N_2)^{2-}$ ligand. Protonation of the coordinated dinitrogen in these complexes gave rise to the formation of ammonia and hydrazine, whereas migration of a Me group from the group 4 or 5 metal center to the dinitrogen ligand has not been observed. The lability of the chloro ligands on the titanium atom in **5a** also enabled us to obtain the sulfur-rich bridging dinitrogen complex **17**, which is a rare example of μ-N_2 complexes with sulfur donor ligands and is interesting in relevalence to the metal−sulfur multinuclear structure in the active site of nitrogenase. Further study on the chemical transformation of the μ-N_2 ligand in the group 6−group 4 or 5 heterodinuclear complexes is under way.

Experimental Section

General Procedure. All reactions were carried out under a dry nitrogen atmosphere unless otherwise noted. Solvents were dried by usual methods and distilled before use. Li_2S_5[44] and complexes **1**,[45] **2a**,[45] **2b**,[46] **7**,[30] $[Cp_2ZrMeCl]$,[47] $[Cp^*NbCl_4]$,[48] $[CpTaCl_4]$,[49] $[Me_3TaCl_2]$,[50] and $[Me_2NbCl_3]$[51] were prepared according to the literature methods. Other reagents were commercially obtained and used without further purification.

^1H and $^{31}P\{^1H\}$ NMR spectra were recorded on a JEOL JNM-EX-270 (^1H, 270 MHz; ^{31}P, 109 MHz) or JEOL JNM-LA-400 (^1H, 400 MHz; ^{31}P, 162 MHz) spectrometer. IR spectra were recorded on a Shimadzu FTIR-8100M spectrophotometer. Quantitative GLC analyses were carried out on a Shimadzu GC-8A instrument equipped with a thermal conductivity

---

(39) Glassman, T. E.; Liu, A. H.; Schrock, R. R. *Inorg. Chem.* **1991**, *30*, 4723−4732.

(40) Chatt, J.; Fay, R. C.; Richards, R. L. *J. Chem. Soc., A* **1971**, 702.

(41) Cummins, C. C. *Chem. Commun.* **1998**, 1777−1786.

(42) Laplaza, C. E.; Johnson, M. J. A.; Peters, J. C.; Odom, A. L.; Kim, E.; Cummins, C. C.; George, G. N.; Pickering, I. J. *J. Am. Chem. Soc.* **1996**, *118*, 8623−8638.

(43) Laplaza, C. E.; Johnson, A. R.; Cummins, C. C. *J. Am. Chem. Soc.* **1996**, *118*, 709−710.

(44) Shaver, A.; Mccall, J. M.; Marmolejo, G. *Inorg. Synth.* **1990**, *27*, 59−65.

(45) Chatt, J.; Heath, G. A.; Richards, R. L. *J. Chem. Soc., Dalton Trans.* **1974**, 2074−2082.

(46) Dilworth, J. R.; Richards, R. L.; Chen, G. J.-J.; MacDonald, J. W. *Inorg. Synth.* **1980**, *20*, 119−127.

(47) Jordan, R. F. *J. Organomet. Chem.* **1985**, *294*, 321−326.

(48) Okamoto, T.; Yasuda, H.; Nakamura, A.; Kai, Y.; Kanehisa, N.; Kasai, N. *J. Am. Chem. Soc.* **1988**, *110*, 5008−5017.

(49) Cardoso, A. M.; Clark, R. J. H.; Moorhouse, S. *J. Chem. Soc., Dalton Trans.* **1980**, 1156−1160.

(50) Schrock, R. R.; Sharp, P. R. *J. Am. Chem. Soc.* **1978**, *100*, 2389−2399.

(51) Fowles, G. W. A.; Rice, D. A.; Winkins, J. D. *J. Chem. Soc., Dalton Trans.* **1972**, 2313−2318.

detector using a Molecular Sieve 13X column. Elemental analyses were performed with a Perkin-Elmer 2400 series II CHN analyzer.

Preparation of [WCl(PMe_2Ph)$_4$(μ-N_2)TiCp$_2$Cl] (3a). Complex **1** (500.0 mg, 0.631 mmol) and [Cp_2TiCl_2] (157.0 mg, 0.631 mmol) were dissolved in benzene (12.5 mL) at room temperature, and the mixture was stirred for 17 h at 50 °C. Then the solution was concentrated to ca. 6 mL under vacuum at room temperature. Layering the benzene solution with hexane afforded **3a** as a black solid, which was collected, washed with hexane, and dried in vacuo (466.0 mg, 73% yield): ^{1}H NMR (C_6D_6) δ 1.57 (s, 24H, PMe), 6.30 (s, 10H, Cp), 6.98−7.54 (m, 20H, Ph); IR (KBr) 1468 (m) cm^{-1}. Anal. Calcd for $C_{42}H_{54}Cl_2N_2P_4TiW$: C, 49.78; H, 5.37; N, 2.76. Found: C, 49.40; H, 5.61; N, 2.53.

Preparation of [WI(PMe_2Ph)$_4$(μ-N_2)ZrCp$_2$Cl]·0.5C_6H_6 (3b·0.5C_6H_6), [WI(PMe_2Ph)$_3$(py)(μ-N_2)ZrCp$_2$Cl]·0.5py (3b′·0.5py), and [WI(PMe_2Ph)$_4$(μ-N_2)HfCp$_2$Cl]·C_6H_6 (3c·C_6H_6). Complex **1** (200.0 mg, 0.252 mmol), [Cp_2ZrCl_2] (73.8 mg, 0.252 mmol), and NaI (550.0 mg, 3.70 mmol) were dissolved in benzene (5 mL) at room temperature, and the mixture was stirred for 16 h at 50 °C under dark. Then the solution was cooled to room temperature and filtered. Layering the filtered solution with hexane afforded **3b**·0.5C_6H_6 as a dark red solid, which was collected, washed with hexane, and dried in vacuo (192.0 mg, 64% yield): ^{1}H NMR (C_6D_6) δ 1.71 (s, 24H, PMe), 6.33 (s, 10H, Cp), 6.98−7.48 (m, 20H, Ph); IR (KBr) 1518 (m) cm^{-1}. Anal. Calcd for $C_{45}H_{57}ClIN_2P_4WZr$: C, 45.52; H, 4.84; N, 2.36. Found: C, 45.59; H, 4.89; N, 2.22.

The pyridine complex [WI(PMe_2Ph)$_3$(py)(μ-N_2)ZrCp$_2$Cl]·0.5py (**3b′**·0.5py) was obtained in 44% yield by dissolving complex **3b**·0.5C_6H_6 in pyridine followed by addition of hexane to the pyridine solution and further recrystallization of the solid deposited from toluene−pyridine/hexane. ^{1}H NMR (C_4D_8O): δ 1.50 (t, 6H, J = 2.7 Hz, trans PMe), 1.59 (t, 6H, J = 2.7 Hz, trans PMe), 1.90 (d, 6H, J = 6.0 Hz, unique PMe), 6.24 (s, 10H, Cp), 6.82−7.41 (m, 15H, Ph). This complex is somewhat unstable in solution, and signals of the pyridine ligand were obscured by overlapping with those of decomposition products. IR (KBr): 1541 (m) cm^{-1}. Anal. Calcd for $C_{41.5}H_{50.5}ClIN_{3.5}P_3WZr$: C, 44.16; H, 4.51; N, 4.34. Found: C, 44.62; H, 4.56; N, 4.30.

Complex **3c**·C_6H_6 was prepared from **1**, [Cp_2HfCl_2], and NaI as a brown solid in 60% yield by a procedure similar to that described for complex **3b**·0.5C_6H_6. ^{1}H NMR (C_6D_6): δ 1.77 (s, 24H, PMe), 6.29 (s, 10H, Cp), 6.99−7.70 (m, 20H, Ph); IR (KBr) 1545 (m) cm^{-1}. Anal. Calcd for $C_{48}H_{66}ClHfIN_2P_4W$: C, 43.89; H, 4.60; N, 2.13. Found: C, 43.85; H, 4.63; N, 2.08.

Preparation of [WCl(PMe_2Ph)$_4$(μ-N_2)TiCpCl$_2$] (4). Complex **1** (225.2 mg, 0.284 mmol) and [$CpTiCl_3$] (62.2 mg, 0.284 mmol) were dissolved in benzene (5 mL) at room temperature. With rapid evolution of nitrogen gas, the color of the solution immediately changed from orange to dark green. The mixture was stirred for a further 8 h, and the solvent was evaporated under vacuum to give a dark green solid. The residual solid was dissolved in CH_2Cl_2, and the solution was filtered. Layering the CH_2Cl_2 solution with ether afforded black crystals of **4**, which were collected, washed with ether, and dried in vacuo (196.0 mg, 70% yield): ^{1}H NMR ($CDCl_3$) δ 1.63 (s, 24H, PMe), 6.44 (s, 5H, Cp), 7.27−7.46 (m, 20H, Ph); ^{31}P{^{1}H} NMR ($CDCl_3$) δ −24.5 (s with ^{183}W satellites, J_{WP} = 277 Hz); IR (KBr) 1408 (m) cm^{-1}. Anal. Calcd for $C_{37}H_{49}Cl_3N_2P_4TiW$: C, 45.17; H, 5.02; N, 2.85. Found: C, 45.50; H, 5.29; N, 2.70.

Preparation of [WCl(dppe)$_2$(μ-N_2)TiCpCl$_2$]·CH_2Cl_2·Et_2O (5a·CH_2Cl_2·Et_2O) and [MoCl(dppe)$_2$(μ-N_2)TiCpCl$_2$] (5b). Complex **2a** (198.0 mg, 0.191 mmol) and [$CpTiCl_3$] (41.9 mg, 0.191 mmol) were dissolved in THF (5 mL) at room temperature. With rapid evolution of nitrogen gas, the color of the solution changed from orange to dark green. The mixture was stirred for a further 8 h, and the solvent was evaporated to give a dark green solid. The residual solid was dissolved in CH_2Cl_2, and the solution was filtered. Layering the CH_2Cl_2 solution with ether afforded black crystals of **5a**·CH_2Cl_2·Et_2O, which were collected, washed with ether, and dried in vacuo (166.2 mg, 63% yield): ^{1}H NMR ($CDCl_3$) δ 2.46, 2.89 (br, 4H each, CH_2 of dppe), 5.70 (s, 5H, Cp), 6.66−7.67 (m, 40H, Ph); ^{31}P{^{1}H} NMR ($CDCl_3$) δ 36.0 (s with ^{183}W satellites, J_{WP} = 284 Hz); IR (KBr) 1412 (m) cm^{-1}. Anal. Calcd for $C_{62}H_{65}Cl_5N_2OP_4TiW$: C, 53.69; H, 4.72; N, 2.02. Found: C, 53.49; H, 4.60; N, 2.19.

Complex **5b** was prepared from **2b** and [$CpTiCl_3$] as black crystals in 78% yield by a procedure similar to that described for complex **5a**·CH_2Cl_2·Et_2O: ^{1}H NMR ($CDCl_3$) δ 2.31, 2.66 (br, 4H each, CH_2 of dppe), 5.73 (s, 5H, Cp), 6.78−7.77 (m, 40H, Ph); ^{31}P{^{1}H} NMR ($CDCl_3$) δ 52.9 (s); IR (KBr) 1416 (m) cm^{-1}. Anal. Calcd for $C_{57}H_{53}Cl_3MoN_2P_4Ti$: C, 60.05; H, 4.69; N, 2.46. Found: C, 60.13; H, 5.06; N, 2.22.

Preparation of [W(OTf)(PMe_2Ph)$_4$(μ-N_2)TiCp$_2$(OTf)] (6a). Complex **1** (120.1 mg, 0.152 mmol) and [$Cp_2Ti(OTf)_2$] (72.2 mg, 0.152 mmol) were dissolved in benzene (3 mL) at room temperature. With rapid evolution of nitrogen gas, the color of the solution immediately changed from orange to black. The mixture was stirred for further 30 min and filtered. Addition of hexane to the filtrate afforded **6a** as a brown solid (181.3 mg, 96% yield): ^{1}H NMR (C_6D_6) δ 1.51 (s, 24H, PMe), 6.21 (s, 10H, Cp), 6.98−7.23 (m, 20H, Ph); ^{31}P{^{1}H} NMR (C_6D_6) δ −25.4 (s with ^{183}W satellites, J_{WP} = 290 Hz); IR (KBr) 1555 (m) cm^{-1}. Anal. Calcd for $C_{44}H_{54}F_6N_2O_6P_4S_2TiW$: C, 42.60; H, 4.39; N, 2.26. Found: C, 42.90; H, 4.59; N, 2.23.

Preparation of [W(OTf)(dppe)$_2$(μ-N_2)TiCp$_2$(OTf)] (6b). Complex **2a** (172.0 mg, 0.166 mmol) and [$Cp_2Ti(OTf)_2$] (79.0 mg, 0.166 mmol) were dissolved in benzene (3 mL) at room temperature. With rapid evolution of nitrogen gas, the color of the solution changed from orange to black, and a black solid began to precipitate. The suspension was stirred for further 30 min, and the solvent was evaporated under vacuum to give a black solid. The residual solid was dissolved in THF, and the solution was filtered. Layering the THF solution with hexane afforded **6b** as a brown solid (151.6 mg, 88% yield): ^{1}H NMR (C_4D_8O) δ 2.60, 3.10 (br, 4H each, CH_2 of dppe), 5.91 (s, 10H, Cp), 6.68−7.52 (m, 40H, Ph); ^{31}P{^{1}H} NMR (C_4D_8O) δ 41.4 (s with ^{183}W satellites, J_{WP} = 297 Hz); IR (KBr) 1545 (m) cm^{-1}. Anal. Calcd for $C_{64}H_{58}F_6N_2O_6P_4S_2TiW$: C, 51.77; H, 3.94; N, 1.89. Found: C, 52.03; H, 4.33; N, 2.12.

Preparation of [W(NCS)(dppe)$_2$(μ-N_2)TiCp$_2$Cl]·CH_2Cl_2 (8a·CH_2Cl_2), [W(NCS)(dppe)$_2$(μ-N_2)ZrCp$_2$Cl]·CH_2Cl_2 (8b·CH_2Cl_2), and [W(NCS)(dppe)$_2$(μ-N_2)HfCp$_2$Cl]·0.5CH_2Cl_2 (8c·0.5CH_2Cl_2). Complex **7** (110.4 mg, 0.084 mmol) and [Cp_2TiCl_2] (21.0 mg, 0.084 mmol) were dissolved in benzene (3 mL), and the mixture was stirred for 10 h at room temperature. During this period, the color of the solution gradually changed from black to dark red. Then the reaction mixture was evaporated under vacuum to give a black solid. The residual solid was dissolved in CH_2Cl_2, and the solution was filtered. Layering the CH_2Cl_2 solution with hexane afforded black crystals of **8a**·CH_2Cl_2, which were collected, washed with hexane, and dried in vacuo (71.0 mg, 62% yield): ^{1}H NMR ($CDCl_3$) δ 2.54, 2.95 (br, 4H each, CH_2 of dppe), 5.65 (s, 10H, Cp), 6.44−7.55 (m, 40H, Ph); ^{31}P{^{1}H} NMR ($CDCl_3$) δ 37.9 (s with ^{183}W satellites, J_{WP} = 288 Hz); IR (KBr) 2049 (s), 1545 (m) cm^{-1}. Anal. Calcd for $C_{64}H_{60}Cl_3N_3P_4STiW$: C, 56.31; H, 4.43; N, 3.08. Found: C, 56.01; H, 4.54; N, 2.75.

The zirconium analogue **8b**·CH_2Cl_2 was prepared from **7** and [Cp_2ZrCl_2] by a procedure similar to that described for complex **8a**·CH_2Cl_2 and isolated as black crystals in 65% yield: ^{1}H NMR ($CDCl_3$) δ 2.41, 2.77 (br, 4H each, CH_2 of dppe), 5.85 (s, 10H, Cp), 6.49−7.66 (m, 40H, Ph); ^{31}P{^{1}H} NMR ($CDCl_3$) δ 44.6 (s with ^{183}W satellites, J_{WP} = 292 Hz); IR (KBr) 2056 (s), 1549 (m) cm^{-1}. Anal. Calcd for $C_{64}H_{60}Cl_3N_3P_4SWZr$: C, 54.57; H, 4.29; N, 2.98. Found: C, 54.17; H, 4.51; N, 2.92.

The hafnium analogue **8c**·0.5CH_2Cl_2 was prepared similarly from **7** and [Cp_2HfCl_2] and isolated as black crystals in 66%

yield: ^{1}H NMR (CDCl$_3$) δ 2.17, 2.56 (br, 4H each, CH$_2$ of dppe), 5.60 (s, 10H, Cp), 6.66−7.50 (m, 40H, Ph); ^{31}P{^{1}H} NMR (CDCl$_3$) δ 47.2 (s with ^{183}W satellites, J_{WP} = 286 Hz); IR (KBr) 2056 (s), 1559 (m) cm^{-1}. Anal. Calcd for C$_{63.5}$H$_{59}$Cl$_2$HfN$_3$P$_4$SW: C, 52.48; H, 4.09; N, 2.89. Found: C, 52.44; H, 4.36; N, 2.55.

Preparation of [W(NCS)(dppe)$_2$(μ-N$_2$)TiCpCl$_2$]·3CH$_2$Cl$_2$ (9a·3CH$_2$Cl$_2$) and [W(NCS)(dppe)$_2$(μ-N$_2$)TiCp*Cl$_2$] (9b). Complex **7** (109.7 mg, 0.084 mmol) and [CpTiCl$_3$] (18.4 mg, 0.084 mmol) were dissolved in benzene (3 mL), and the mixture was stirred for 17 h at room temperature. The resulting reaction mixture was evaporated under vacuum to give a green solid. The residual solid was dissolved in CH$_2$Cl$_2$, and the solution was filtered. Layering the CH$_2$Cl$_2$ solution with ether afforded dark green crystals of **9a**·3CH$_2$Cl$_2$, which were collected, washed with ether, and dried in vacuo (68.0 mg, 54% yield): ^{1}H NMR (CDCl$_3$) δ 2.49, 2.81 (br, 4H each, CH$_2$ of dppe), 5.80 (s, 5H, Cp), 6.55−7.63 (m, 40H, Ph); ^{31}P{^{1}H} NMR (CDCl$_3$) δ 38.2 (s with ^{183}W satellites, J_{WP} = 284 Hz); IR (KBr) 2041 (s), 1441 (m) cm^{-1}. Anal. Calcd for C$_{61}$H$_{59}$Cl$_8$N$_3$P$_4$STiW: C, 48.67; H, 3.95; N, 2.79. Found: C, 49.02; H, 3.77; N, 2.88.

Complex **9b** was prepared from **7** and [Cp*TiCl$_3$] as dark green crystals in 64% yield by a similar procedure except that **9b** was isolated by recrystallization from ClCH$_2$CH$_2$Cl/hexane: ^{1}H NMR (C$_6$D$_6$) δ 1.90 (s, 15H, Cp*), 2.19, 2.58 (br, 4H each, CH$_2$ of dppe), 6.63−7.88 (m, 40H, Ph); ^{31}P{^{1}H} NMR (C$_6$D$_6$) δ 44.3 (s with ^{183}W satellites, J_{WP} = 286 Hz); IR (KBr) 2041 (s), 1433 (m) cm^{-1}. Anal. Calcd for C$_{63}$H$_{63}$Cl$_2$N$_3$P$_4$STiW: C, 57.29; H, 4.81; N, 3.18. Found: C, 57.19; H, 4.79; N, 3.16.

Preparation of [WCl(PMe$_2$Ph)$_4$(μ-N$_2$)NbCpCl$_3$]·CH$_2$Cl$_2$·Et$_2$O (10a·CH$_2$Cl$_2$·Et$_2$O), [WCl(PMe$_2$Ph)$_4$(μ-N$_2$)NbCp*Cl$_3$]·C$_7$H$_8$ (10b·C$_7$H$_8$), [WCl (PMe$_2$Ph)$_4$(μ-N$_2$)TaCpCl$_3$]·CH$_2$Cl$_2$ (10c·CH$_2$Cl$_2$), and [WCl(PMe$_2$Ph)$_4$(μ-N$_2$)TaCp*Cl$_3$] (10d). Complex **1** (4.20 g, 5.30 mmol) and [CpNbCl$_4$] (1.59 g, 5.30 mmol) were dissolved in benzene (20 mL) at room temperature. With rapid evolution of nitrogen gas, the color of the solution changed from orange to black. The mixture was stirred for a further 30 min and evaporated under vacuum to give a black oil. The residual oil was dissolved in CH$_2$Cl$_2$, and the solution was filtered. Layering the CH$_2$Cl$_2$ solution with ether afforded black crystals of **10a**·CH$_2$Cl$_2$·Et$_2$O, which were collected, washed with ether, and dried in vacuo (5.48 g, 85% yield): ^{1}H NMR (CDCl$_3$) δ 1.61 (s, 24H, PMe), 6.37 (s, 5H, Cp), 7.12−7.48 (m, 20H, Ph); ^{31}P{^{1}H} NMR (CDCl$_3$) δ −27.7 (s with ^{183}W satellites, J_{WP} = 273 Hz); IR (KBr) 1395 (m) cm^{-1}. Anal. Calcd for C$_{42}$H$_{61}$Cl$_6$N$_2$NbOP$_4$W: C, 41.24; H, 5.03; N, 2.29. Found: C, 40.99; H, 4.84; N, 2.09.

Complex **10b**·C$_7$H$_8$ was obtained in 98% yield as a dark green powder by the reaction of **1** with [Cp*NbCl$_4$] and recrystallization from toluene/hexane: ^{1}H NMR (C$_6$D$_6$) δ 1.56 (s, 24H, PMe), 2.26 (s, 15H, Cp*), 6.97−7.57 (m, 20H, Ph); ^{31}P{^{1}H} NMR (C$_6$D$_6$) δ −27.3 (s with ^{183}W satellites, J_{WP} = 275 Hz); IR (KBr) 1385 (m) cm^{-1}. Anal. Calcd for C$_{49}$H$_{67}$Cl$_4$N$_2$NbP$_4$W: C, 47.98; H, 5.51; N, 2.28. Found: C, 47.89; H, 5.65; N, 2.04.

Complex **10c**·CH$_2$Cl$_2$ was obtained in 74% yield as a dark red powder by the reaction of **1** with [CpTaCl$_4$] followed by recrystallization from CH$_2$Cl$_2$/hexane: ^{1}H NMR (CDCl$_3$) δ 1.65 (s, 24H, PMe), 6.41 (s, 5H, Cp), 7.31−7.46 (m, 20H, Ph); ^{31}P{^{1}H} NMR (CDCl$_3$) δ −24.6 (s with ^{183}W satellites, J_{WP} = 275 Hz); IR (KBr) 1435 (m) cm^{-1}. Anal. Calcd for C$_{38}$H$_{51}$Cl$_6$N$_2$P$_4$TaW: C, 36.89; H, 4.15; N, 2.26. Found: C, 37.08; H, 4.27; N, 2.29.

Complex **10d** was obtained in 95% yield as a dark red powder by the reaction of **1** with [Cp*TaCl$_4$] followed by recrystallization from toluene/hexane: ^{1}H NMR (C$_6$D$_6$) δ 1.57 (s, 24H, PMe), 2.38 (s, 15H, Cp*), 6.98−7.42 (m, 20H, Ph); ^{31}P{^{1}H} NMR (C$_6$D$_6$) δ −24.9 (s with ^{183}W satellites, J_{WP} = 277 Hz); IR (KBr) 1426 (m) cm^{-1}. Anal. Calcd for C$_{42}$H$_{59}$Cl$_4$N$_2$P$_4$TaW: C, 41.27; H, 4.86; N, 2.29. Found: C, 41.65; H, 5.09; N, 2.21. Dark red crystals of **10d**·2MeCN suitable for the crystallographic study were obtained by recrystallization of **10d** from CH$_2$Cl$_2$−MeCN/ether.

Preparation of [WCl(dppe)$_2$(μ-N$_2$)NbCpCl$_3$]·Et$_2$O (11a·Et$_2$O) and [WCl(dppe)$_2$(μ-N$_2$)TaCpCl$_3$] (11b). Complex **2a** (164.6 mg, 0.159 mmol) and [CpNbCl$_4$] (47.6 mg, 0.159 mmol) were dissolved in THF (5 mL) at room temperature. With rapid evolution of nitrogen gas, the color of the solution immediately changed from orange to black. The mixture was stirred for a further 1 h, and the solvent was evaporated under vacuum to give a dark green solid. The residual solid was dissolved in CH$_2$Cl$_2$, and the solution was filtered. Slow diffusion of ether into the filtrate deposited black crystals of **11a**·Et$_2$O (164.8 mg, 75% yield): ^{1}H NMR (CDCl$_3$) δ 2.68, 2.90 (br, 4H each, CH$_2$ of dppe), 5.86 (s, 5H, Cp), 6.67−7.66 (m, 40H, Ph); ^{31}P{^{1}H} NMR (CDCl$_3$) δ 34.1 (s with ^{183}W satellites, J_{WP} = 275 Hz); IR (KBr) 1383 (m) cm^{-1}. Anal. Calcd for C$_{61}$H$_{63}$Cl$_4$N$_2$NbOP$_4$W: C, 52.99; H, 4.59; N, 2.03. Found: C, 52.88; H, 4.22; N, 2.32.

Complex **11b** was prepared similarly from **2a** and [CpTaCl$_4$] as a brown powder in 46% yield: ^{1}H NMR (CDCl$_3$) δ 2.61, 2.87 (br, 4H each, CH$_2$ of dppe), 5.86 (s, 5H, Cp), 6.68−7.69 (m, 40H, Ph); ^{31}P{^{1}H} NMR (CDCl$_3$) δ 36.9 (s with ^{183}W satellites, J_{WP} = 281 Hz); IR (KBr) 1419 (m) cm^{-1}. Anal. Calcd for C$_{57}$H$_{53}$Cl$_4$N$_2$P$_4$TaW: C, 49.02; H, 3.83; N, 2.01. Found: C, 49.03; H, 4.02; N, 1.64.

Preparation of [W(NCS)(dppe)$_2$(μ-N$_2$)NbCpCl$_3$]·THF (12a·THF) and [W(NCS)(dppe)$_2$(μ-N$_2$)TaCpCl$_3$] (12b). Complex **7** (186.1 mg, 0.142 mmol) and [CpNbCl$_4$] (42.6 mg, 0.142 mmol) were dissolved in THF (3 mL), and the mixture was stirred for 1 h at room temperature. The resulting solution was filtered, and layering the THF solution with hexane afforded black crystals of **12a**·THF (179.0 mg, 90% yield): ^{1}H NMR (CD$_2$Cl$_2$) δ 2.64, 2.83 (br, 4H each, CH$_2$ of dppe), 5.84 (s, 5H, Cp), 6.55−7.60 (m, 40H, Ph); ^{31}P{^{1}H} NMR (CD$_2$Cl$_2$) δ 35.5 (s with ^{183}W satellites, J_{WP} = 277 Hz); IR (KBr) 2029 (s), 1395 (m) cm^{-1}. Anal. Calcd for C$_{62}$H$_{61}$Cl$_3$N$_3$NbOP$_4$SW: C, 53.07; H, 4.38; N, 2.99. Found: C, 52.89; H, 4.24; N, 3.28.

Complex **12b** was prepared in 98% yield as a dark red powder by the reaction of **7** with [CpTaCl$_4$] followed by recrystallization from toluene/hexane: ^{1}H NMR (CD$_2$Cl$_2$) δ 2.55, 2.89 (br, 4H each, CH$_2$ of dppe), 5.96 (s, 5H, Cp), 6.60−7.61 (m, 40H, Ph); ^{31}P{^{1}H} NMR (CD$_2$Cl$_2$) δ 37.4 (s with ^{183}W satellites, J_{WP} = 281 Hz); IR (KBr) 2037 (s), 1420 (m) cm^{-1}. Anal. Calcd for C$_{58}$H$_{53}$Cl$_3$N$_3$P$_4$STaW: C, 49.09; H, 3.76; N, 2.96. Found: C, 49.02; H, 3.89; N, 2.67.

Preparation of [WCl(PMe$_2$Ph)$_3$(^{t}BuNC)(μ-N$_2$)TaCp*Cl$_3$] (13). Complex **9d** (177.0 mg, 0.145 mmol) and ^{t}BuNC (70.1 mg, 0.236 mmol) were dissolved in ClCH$_2$CH$_2$Cl (3 mL), and the mixture was stirred for 10 h at 50 °C. The resulting solution was evaporated under vacuum, and the residual dark red solid was dissolved in toluene. Slow diffusion of hexane into the filtrated toluene solution deposited a red powder of **12** (44.0 mg, 26% yield): ^{1}H NMR (C$_6$D$_6$) δ 0.95 (s, 9H, ^{t}Bu), 1.29 (d, 6H, J = 7.8 Hz, unique PMe), 1.78 (t, 6H, J = 3.7 Hz, trans PMe), 1.80 (t, 6H, J = 3.9 Hz, trans PMe), 2.30 (s, 15H, Cp*), 6.97−7.67 (m, 15H, Ph); ^{31}P{^{1}H} NMR (C$_6$D$_6$) δ −20.3 (d with ^{183}W satellites, J_{WP} = 297 Hz, $J_{PP'}$ = 11 Hz), −24.4 (t with ^{183}W satellites, J_{WP} = 260 Hz); IR (KBr) 2112 (m), 1458 (m) cm^{-1}. Anal. Calcd for C$_{39}$H$_{57}$Cl$_4$N$_3$P$_3$TaW: C, 40.12; H, 4.92; N, 3.60. Found: C, 40.34; H, 5.17; N, 3.98.

Preparation of [WI(PMe$_2$Ph)$_4$(μ-N$_2$)ZrCp$_2$Me] (14a). Complex **1** (182.1 mg, 0.230 mmol), [Cp$_2$ZrMeCl] (62.5 mg, 0.230 mmol), and NaI (418 mg, 2.79 mmol) were dissolved in toluene (5 mL), and the mixture was stirred for 20 h at 50 °C. The resulting reaction mixture was filtered, and the solvent was evaporated under vacuum to give a black solid. Recrystallization from CH$_2$Cl$_2$/hexane afforded **14a** as a brown powder, which was collected, washed with hexane, and dried in vacuo (128.6 mg, 31% yield): ^{1}H NMR (C$_6$D$_6$) δ 0.37 (s, 3H, ZrMe), 1.67 (s, 24H, PMe), 6.11 (s, 10H, Cp), 6.79−7.58 (m, 20H, Ph); ^{31}P{^{1}H} NMR (C$_6$D$_6$) δ −31.8 (s with ^{183}W satellites,

J_{WP} = 290 Hz); IR (KBr) 1541 (m) cm^{-1}. Anal. Calcd for $C_{43}H_{57}IN_2P_4WZr$: C, 45.79; H, 5.09; N, 2.48. Found: C, 45.42; H, 5.33; N, 2.72.

Preparation of [W(NCS)(dppe)$_2$(μ-N$_2$)ZrCp$_2$Me] (14b). Complex **7** (225.0 mg, 0.172 mmol) and [Cp$_2$ZrMeCl] (46.9 mg, 0.172 mmol) were dissolved in benzene (5 mL), and the mixture was stirred for 1 h at room temperature. Then the reaction mixture was evaporated under vacuum, and the residual black solid was extracted with THF. Layering the THF solution with hexane afforded black crystals of **14b** (196.7 mg, 88% yield): ^{1}H NMR (CDCl$_3$) δ −0.02 (s, 3H, ZrMe), 2.32, 2.68 (br, 4H each, CH$_2$ of dppe), 5.66 (s, 10H, Cp), 6.48−7.66 (m, 40H, Ph); ^{31}P{^{1}H} NMR (CDCl$_3$) δ 45.8 (s with ^{183}W satellites, J_{WP} = 297 Hz); IR (KBr) 2060 (s), 1557 (m) cm^{-1}. Anal. Calcd for $C_{64}H_{61}N_3P_4SWZr$: C, 58.98; H, 4.72; N, 3.22. Found: C, 58.82; H, 4.63; N, 3.12.

Preparation of [WCl(PMe$_2$Ph)$_4$(μ-N$_2$)TaMe$_3$Cl] (15a), [WCl(dppe)$_2$(μ-N$_2$)TaMe$_3$Cl] (15b), and [MoCl(dppe)$_2$(μ-N$_2$)TaMe$_3$Cl] (15c). Complex **1** (187.0 mg, 0.236 mmol) and [Me$_3$TaCl$_2$] (70.1 mg, 0.236 mmol) were dissolved in toluene (3 mL) at room temperature. With rapid evolution of nitrogen gas, the color of the solution changed from orange to black. The mixture was stirred for a further 30 min and filtered. Layering the filtrate with hexane afforded **15a** as a brown powder, which was collected, washed with hexane, and dried in vacuo (165.7 mg, 66% yield): ^{1}H NMR (C$_4$D$_8$O) δ 0.45 (s, 9H, TaMe), 1.68 (s, 24H, PMe), 6.94−7.44 (m, 20H, Ph); ^{31}P{^{1}H} NMR (C$_4$D$_8$O) δ −19.9 (s with ^{183}W satellites, J_{WP} = 278 Hz); IR (KBr) 1480 (m) cm^{-1}. Anal. Calcd for $C_{35}H_{53}Cl_2N_2P_4TaW$: C, 39.61; H, 5.03; N, 2.64. Found: C, 40.00; H, 4.84; N, 2.29.

Complex **15b** was prepared similarly from **2a** and [Me$_3$TaCl$_2$] in 55% yield: ^{1}H NMR (C$_4$D$_8$O) δ 0.23 (s, 9H, TaMe), 2.41, 2.99 (br, 4H each, CH$_2$ of dppe), 6.73−7.75 (m, 40H, Ph); ^{31}P{^{1}H} NMR (C$_4$D$_8$O) δ 42.0 (s with ^{183}W satellites, J_{WP} = 290 Hz); IR (KBr) 1470 (m) cm^{-1}. Anal. Calcd for $C_{55}H_{57}Cl_2N_2P_4TaW$: C, 50.60; H, 4.40; N, 2.15. Found: C, 50.55; H, 4.02; N, 1.99.

Complex **15c** was prepared in 59% yield as a black powder by the reaction of with **2b** with [Me$_3$TaCl$_2$] and recrystallization from CH$_2$Cl$_2$/hexane: ^{1}H NMR (C$_4$D$_8$O) δ 0.13 (s, 9H, TaMe), 2.46, 2.92 (br, 4H each, CH$_2$ of dppe), 6.73−7.74 (m, 40H, Ph); ^{31}P{^{1}H} NMR (C$_4$D$_8$O) δ 55.5 (s); IR (KBr) 1483 (m) cm^{-1}. Anal. Calcd for $C_{55}H_{57}Cl_2MoN_2P_4Ta$: C, 54.25; H, 4.72; N, 2.30. Found: C, 53.99; H, 4.42; N, 1.93.

Preparation of [WCl(dppe)$_2$(μ-N$_2$)NbMe$_2$Cl$_2$] (16a·CH$_2$Cl$_2$) and [MoCl(dppe)$_2$(μ-N$_2$)NbMe$_2$Cl$_2$] (16b). Complex **2a** (360.8 mg, 0.348 mmol) and [Me$_2$NbCl$_3$] (79.8 mg, 0.348 mmol) were dissolved in benzene (3 mL) at room temperature. With rapid evolution of nitrogen gas, the color of the solution changed from orange to black. The mixture was stirred for a further 30 min, and the solvent was evaporated under vacuum to give a black solid. The residual solid was dissolved in CH$_2$Cl$_2$, and the solution was filtered. Layering the CH$_2$Cl$_2$ solution with hexane afforded black crystals of **16a**·CH$_2$Cl$_2$ (222.2 mg, 48% yield): ^{1}H NMR (C$_6$D$_6$) δ 1.25 (s, 6H, NbMe), 2.28, 2.61 (br, 4H each, CH$_2$ of dppe), 6.79−7.75 (m, 40H, Ph); ^{31}P{^{1}H} NMR (C$_6$D$_6$) δ 35.1 (s with ^{183}W satellites, J_{WP} = 281 Hz); IR (KBr) 1406 (m) cm^{-1}. Anal. Calcd for $C_{55}H_{56}Cl_5N_2NbP_4W$: C, 49.93; H, 4.27; N, 2.12. Found: C, 50.27; H, 4.17; N, 1.73.

Complex **16b** was prepared from **2b** and [Me$_2$NbCl$_3$] as a black powder in 74% yield by a similar procedure except that **16b** was isolated by recrystallization from benzene/hexane: ^{1}H NMR (CDCl$_3$) δ 0.65 (s, 6H, NbMe), 2.44, 2.80 (br, 4H each, CH$_2$ of dppe), 6.71−7.55 (m, 40H, Ph); ^{31}P{^{1}H} NMR (CDCl$_3$) δ 51.5 (s); IR (KBr) 1408 (m) cm^{-1}. Anal. Calcd for $C_{54}H_{54}Cl_3MoN_2NbP_4$: C, 56.39; H, 4.73; N, 2.44. Found: C, 56.50; H, 4.58; N, 2.04.

Preparation of [WCl(dppe)$_2$(μ-N$_2$)TiCpS$_5$]·0.5Et$_2$O (17·0.5Et$_2$O). To a dark yellow solution of Li$_2$S$_5$ prepared from S$_8$ (0.046 mmol) and LiBEt$_3$H (0.147 mmol) in THF (5 mL) was added **5a**·CH$_2$Cl$_2$·Et$_2$O (90.4 mg, 0.065 mmol), and the resultant black solution was stirred for 24 h at room temperature. A brown solid precipitated during this period was filtered off, washed with a small amount of EtOH, and dried in vacuo. Recrystallization of this precipitate from CHCl$_3$/ether deposited black crystals, which were collected, washed with ether, and dried in vacuo to give **17**·0.5Et$_2$O (58.5 mg, 66% yield): ^{1}H NMR (CDCl$_3$) δ 2.50, 2.90 (br, 4H each, CH$_2$ of dppe), 5.61 (s, 5H, Cp), 6.60−7.60 (m, 40H, Ph); ^{31}P{^{1}H} NMR (CDCl$_3$) δ 42.0 (s with ^{183}W satellites, J_{WP} = 290 Hz); IR (KBr) 1406 (m) cm^{-1}. Anal. Calcd for $C_{59}H_{58}ClN_2O_{0.5}P_4S_5TiW$: C, 52.32; H, 4.32; N, 2.07. Found: C, 52.20; H, 4.63; N, 2.08. X-ray diffraction study of the crystalline sample clearly indicated that it contains 1.5 molecules of ether per one molecule of **17**, but the crystals gave off a part of the ether molecules on drying under vacuum to give a sample with the empirical formula of **17**·0.5Et$_2$O.

Reaction of the Heterobimetallic Dinitrogen Complexes with H$_2$SO$_4$. In a typical run, concentrated H$_2$SO$_4$ (10 equiv) was added to a suspension of **10d** (95.8 mg, 0.078 mmol) in MeOH (3 mL) under argon, and the mixture was stirred at room temperature for 3 h. The gaseous phase was analyzed by GLC, which showed that essentially no dinitrogen gas was evolved. Then the solution was dried up, and the amounts of ammonia and hydrazine included in the residue were determined as described previously.[52]

Crystallography. Single crystals of **4**, **9a**·3CH$_2$Cl$_2$, **10a**·CH$_2$Cl$_2$·Et$_2$O, **10d**·2MeCN, **11a**·Et$_2$O, **14b**, and **17**·1.5Et$_2$O suitable for X-ray analyses were sealed in Pyrex glass capillaries under an argon atmosphere and used for data collection. Diffraction data were collected on a Rigaku AFC-7R four-circle automated diffractometer with Mo Kα (λ = 0.71069 Å) radiation and a graphite monochromator at 21 °C using the $\omega-2\theta$ scan technique. Empirical absorption correction based on ψ scans and Lorentz−polarization correction were applied. For compounds **9a**·3CH$_2$Cl$_2$, **10a**·CH$_2$Cl$_2$·Et$_2$O, **10d**·2MeCN, **11a**·Et$_2$O, and **14b**, decay (17.57, 3.35, 17.33, 6.14, and 9.62%, respectively) was observed during the data collection, and a correction for decay was applied in each case. Details of the X-ray diffraction study are summarized in Tables 5 and 6. The structure solution and refinements were performed by using the teXsan program package.[53] The positions of the non-hydrogen atoms were determined by direct methods (SIR 92[54] for **9a**·3CH$_2$Cl$_2$) or by Patterson methods (DIRDIF PATTY[55] for the others) and expanded using Fourier techniques. The CH$_2$Cl$_2$ molecules in **9a**·3CH$_2$Cl$_2$, the CH$_2$Cl$_2$ and ether molecules in **10a**·CH$_2$Cl$_2$·Et$_2$O, and the MeCN molecules in **10d**·2MeCN showed signs of disorder and could not be refined satisfactorily. The non-hydrogen atoms of these solvent molecules were found from the difference Fourier maps and included in the refinement with fixed isotropic parameters. One of the ether molecules in **17**·1.5Et$_2$O was found to be located on the center of symmetry. The carbon and oxygen atoms of this ether molecule were included in the refinement as fixed atoms, where the disordered methylene carbon atoms were considered to have the occupancies of 50%. Isotropic thermal parameters were used for the carbon and oxygen atoms of the ether molecule in **11a**·Et$_2$O. All other non-hydrogen atoms were refined by full-matrix least-squares techniques with anisotropic thermal parameters, and the hydrogen atoms except for those of the solvent molecules in

---

[52] Takahashi, T.; Mizobe, Y.; Sato, M.; Uchida, Y.; Hidai, M. *J. Am. Chem. Soc.* **1980**, *102*, 7461−7475.

[53] *teXsan: Crystal Structure Analysis Package*; Molecular Structure Corp.: The Woodlands, TX, 1985 and 1992.

[54] Altomare, A.; Burla, M. C.; Camalli, M.; Cascarano, M.; Giacovazzo, C.; Guagliardi, A.; Polidori, G. *J. Appl. Crystallogr.* **1994**, *27*, 435.

[55] PATTY: Beurskens, P. T.; Admiraal, G.; Beurskens, G.; Bosman, W. P.; Garcia-Granda, S.; Gould, R. O.; Smits, J. M. M.; Smykalla, C. *The DIRDIF program system*; Technical Report of the Crystallography Laboratory; University of Nijmegen: Nijmegen, The Netherlands, 1992.

Table 5. Crystallographic Data for 4, 9a·3CH$_2$Cl$_2$, 10a·CH$_2$Cl$_2$·Et$_2$O, and 10d·2MeCN

	4	**9a**·3CH$_2$Cl$_2$	**10a**·CH$_2$Cl$_2$·Et$_2$O	**10d**·2MeCN
formula	$C_{37}H_{49}Cl_3N_2P_4TiW$	$C_{61}H_{59}Cl_8N_3P_4STiW$	$C_{42}H_{61}Cl_6N_2NbOP_4W$	$C_{46}H_{65}Cl_4N_4P_4TaW$
fw	983.81	1505.49	1223.33	1304.55
space group	Cc	$P\bar{1}$	$P2_1/n$	$P\bar{1}$
a, Å	15.563(2)	12.290(2)	10.753(5)	11.917(2)
b, Å	16.800(1)	13.700(3)	22.320(6)	12.769(3)
c, Å	15.932(2)	20.359(4)	21.467(6)	18.984(3)
α, deg		98.86(2)		87.14(1)
β, deg	92.36(1)	106.33(1)	99.39(4)	89.32(1)
γ, deg		93.63(2)		66.33(1)
V, Å^3	4162.1(8)	3229(1)	5083(3)	2642.4(8)
Z	4	2	4	2
d_{calc}, g cm^{-3}	1.570	1.548	1.598	1.640
μ_{calc}, cm^{-1}	33.31	24.08	29.63	46.01
R^a	0.027	0.068	0.050	0.040
$R_w{}^b$	0.032	0.070	0.061	0.041

[a] $R = \sum||F_o| - |F_c||/\sum|F_o|$. [b] $R_w = [\sum w(F_o| - |F_c|)^2/\sum wF_o{}^2]^{1/2}$, $w = 1/\sigma^2(F_o)$.

Table 6. Crystallographic Data for 11a·Et$_2$O, 14b, and 17·1.5Et$_2$O

	11a·Et$_2$O	**14b**	**17**·1.5Et$_2$O
formula	$C_{61}H_{63}Cl_4N_2NbOP_4W$	$C_{64}H_{61}N_3P_4SWZr$	$C_{63}H_{68}ClN_2O_{1.5}P_4S_5TiW$
fw	1382.65	1303.23	1428.64
space group	$P2_1/n$	$P2_1/a$	$P2_1/n$
a, Å	19.539(4)	17.815(4)	13.531(2)
b, Å	14.883(2)	17.584(4)	18.472(4)
c, Å	20.185(4)	18.606(4)	25.416(2)
β, deg	90.31(2)	95.57(2)	98.477(8)
V, Å^3	5869(1)	5800(2)	6283(1)
Z	4	4	4
d_{calc}, g cm^{-3}	1.564	1.492	1.510
μ_{calc}, cm^{-1}	24.89	23.52	23.12
R^a	0.044	0.037	0.049
$R_w{}^b$	0.047	0.036	0.038

[a] $R = \sum||F_o| - |F_c||/\sum|F_o|$. [b] $R_w = [\sum w(|F_o| - |F_c|)^2/\sum wF_o{}^2]^{1/2}$, $w = 1/\sigma^2(F_o)$.

10a·CH$_2$Cl$_2$·Et$_2$O and the disordered ether molecule in **17**·1.5Et$_2$O were included in the refinements with fixed isotropic parameters.

Acknowledgment. This work was supported by a Grant-in-Aid for Specially Promoted Research (09102004) from the Ministry of Education, Science, Sports, and Culture, Japan.

Supporting Information Available: Tables of atom coordinates, anisotropic thermal parameters, and bond distances and angles for **4**, **9a**·3CH$_2$Cl$_2$, **10a**·CH$_2$Cl$_2$·Et$_2$O, **10d**·2MeCN, **11a**·Et$_2$O, **14b**, and **17**·1.5Et$_2$O. This material is available free of charge via the Internet at http://pubs.acs.org.

OM000684J